Journal of Physics: Conference Series **122** (2008) 012017 doi:10.1088/1742-6596/122/1/012017

Experimental investigation of a control scheme for a tuned resonant sideband extraction interferometer for next-generation gravitational-wave detectors

Fumiko Kawazoe[1], Shuichi Sato[2], Volker Leonhardt[2], Osamu Miyakawa[3], Tomoko Morioka[4], Atsushi Nishizawa[5], Toshitaka Yamazaki[2], Mitsuhiro Fukushima[2], Seiji Kawamura[2], and Akio Sugamoto[1]

[1] Ochanomizu University, 2-1-1 Otsuka, Bunkyo-ku, Tokyo 112-8610, Japan
[2] National Astronomical Observatory of Japan, 2-21-1 Osawa, Mitaka-shi, Tokyo 112-8610, Japan
[3] California Institute of Technology, Pasadena, CA 91125 USA
[4] University of Tokyo, Kashiwa, Chiba 277-8582, Japan
[4] Kyoto University, Yoshida-Honmachi, Sakyo-ku, Kyoto 606-8501, Japan

E-mail: kawazoe@gravity.mtk.nao.ac.jp

Abstract. LCGT plans to use tuned RSE as the optical configuration for its interferometer. A tuned RSE interferometer has five degrees of freedom that need to be controlled in order to operate a gravitational-wave detector, although it is expected to be very challenging because of the complexity of its optical configuration. A new control scheme for a tuned RSE interferometer has been developed and tested with a prototype interferometer to demonstrate successful control of the tuned RSE interferometer. The whole RSE interferometer was successfully locked with the control scheme. Here the control scheme and the current status of the experiment are presented.

1. Introduction

Presently several laser interferometer gravitational-wave detectors, such as LIGO[1], GEO600[2], VIRGO[3], and TAMA300[4], are in operation around the world. In addition to the present detectors, there are plans to upgrade them to next-generation interferometers. Amongst them are Advanced LIGO[5] and LCGT[6], which plan to use the Resonant Sideband Extraction (RSE) technique to enhance detector sensitivities. The LCGT plans to use a tuned RSE configuration while Advanced LIGO plans to use a detuned RSE configuration. Despite the great advantage that it is able to achieve better sensitivity by avoiding problems of thermal absorption by substrates, the RSE configuration poses a more difficult challenge in controlling the interferometer in order to use it as a gravitational-wave detector due to the increased number of degrees of freedom (DOF) that need to be controlled. Therefore, designing a control scheme as simple as possible, and demonstrating it are vital before the technique is adapted in large-scale interferometers such as LCGT. This experiment aims to control a tuned RSE interferometer using the scheme, and to measure the sensing matrix and compare it with modeling. The control

scheme is described in section 2, and the current status of the experiment is presented in section 3.

2. Control of the RSE interferometer

2.1. Degrees of freedom in the RSE interferometer

The RSE interferometer has five DOFs to be controlled as shown in Fig. 1. They are the average length and the differential length of the two Fabry-Perot (FP) cavities, $L+$, and $L-$, respectively, as indicated by red arrows, the average length and the differential length of the power recycling cavity(PRC), $l+$, and $l-$, respectively, as indicated by green arrows, and the average length of the signal extraction cavity(SEC), ls, as indicated by blue arrows.

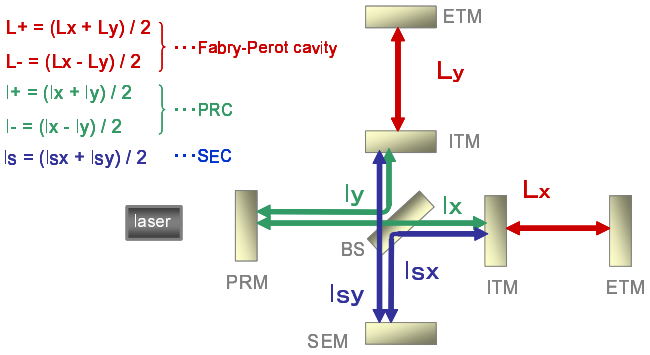

Figure 1. Degrees of freedom in the RSE interferometer.

It is known from experience with present detectors that use the Pound-Drever-Hall (PDH) method that the FP cavities are relatively easy to control with clear control signals as the cavities have high finesse. On the other hand, it is expected to be quite challenging to obtain clear control signals of the central part of the RSE, because the resonant conditions of the light fields inside the central part will be strongly affected by both the PRC, and the SEC, which causes the signals to be strongly coupled. Thus the control scheme has to be designed in such a way that it manipulates the resonant conditions of the light inside by properly designing cavity lengths and sideband frequencies.

2.2. The control scheme

The outline of the control scheme is as follows. It is based on the PDH method. The FP cavity lengths are controlled with a single modulation-demodulation technique and the central part of the RSE is controlled with a double modulation-demodulation technique with amplitude modulation (AM) sidebands and phase modulation (PM) sidebands. By using the double modulation-demodulation technique, the control signals for the central part will be affected very little by the signals derived from the carrier which are dominated by the FP cavities. This is because both the AM and the PM modulation frequencies are designed in such a way that they are not resonant in the FP cavities, thus it decouples the FP cavities and the central part.

2.3. The central part

The central part is designed so that the AM and the PM sidebands behave in the following way. The lengths of two paths that compose the Michelson interferometer have a macroscopic asymmetry such that when the carrier interferes destructively at the dark port (DP), the AM sidebands interfere constructively at the bright port (BP) and destructively at the DP, while

the PM sidebands interferes destructively at the BP and constructively at the DP. Thus the AM sidebands "reflect completely" from the Michelson part while the PM sidebands "transmit completely" through the Michelson part. This condition is met when the round trip Michelson asymmetry length is designed to be equal to $(2m+1)/2$ $(m = 0, 1, 2, ...)$ times the wavelength for the AM sidebands and integer multiple of the wavelength for the PM sidebands. In our design it is 3λ for the AM sidebands and $\frac{1}{2}\lambda$ for the PM sidebands, as shown in Fig. 2. Two

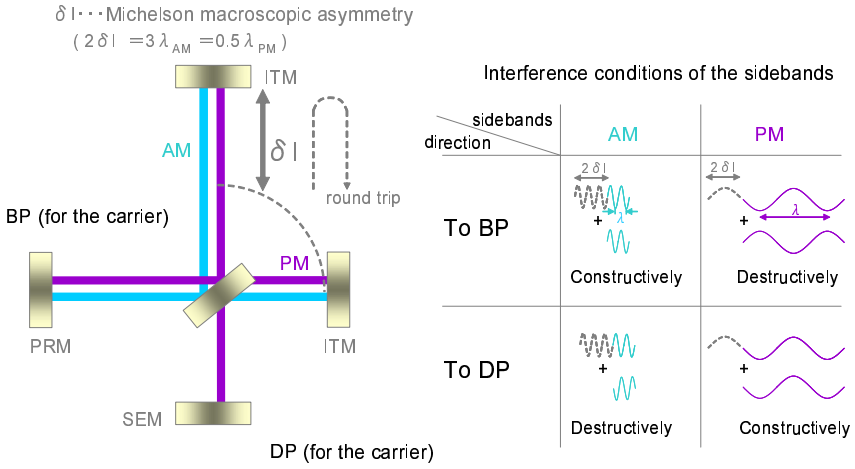

Figure 2. Interference conditions of the two sets of sidebands in the central part of the RSE interferometer.

cavities' macroscopic lengths are designed so that the AM sidebands resonate inside the PRC and the PM sidebands resonate inside the compound cavity made of the PRC and the SEC[7]. This enables the PM sidebands to be sensitive to the length of the SEC while the AM sidebands is not affected by the SEC length, thus ensuring independent control signals for $l+$ and ls.

2.4. Delocation scheme

In addition we have designed an additional scheme to optically diagonalize the control signal matrix[8]. It is expected to provide possible advantages such as a better signal to noise ratio, a simpler lock acquisition process, and a more robust control of the interferometer. It is an optional design for LCGT. The scheme is applied as shown in Fig. 3. The macroscopic position of the power recycling mirror (PRM) and the signal extraction mirror (SEM) is shifted in the direction indicated by red arrows in the figure by the same amount. After the technique is applied, the AM sidebands are off resonant inside the PRC while the PM sidebands stay resonant inside the compound cavity. Due to the slight detuning of the AM sidebands from the resonance, there are changes in proper demodulation phases that give the maximum desired signal at each detection port. The amount by which the mirror positions are shifted is analytically calculated so that it gives the relative shift of $\frac{\pi}{2}$ in the proper demodulation phase for the $l+$ and the ls signals at the PO, where one of the two proper demodulation phases for the $l-$ signal is originally shifted by $\frac{\pi}{2}$ from the other two signals. Therefore the three signals can be diagonalized at the PO. Table 2 shows the optically diagonalized sensing matrix. For comparison, the normalized matrix without the delocation technique is listed on Table 1. Although the three signals can be diagonalized at the PO, in reality l_- should be detected where the ratio between the signal and the shot noise is largest, which is expected to be at the DP.

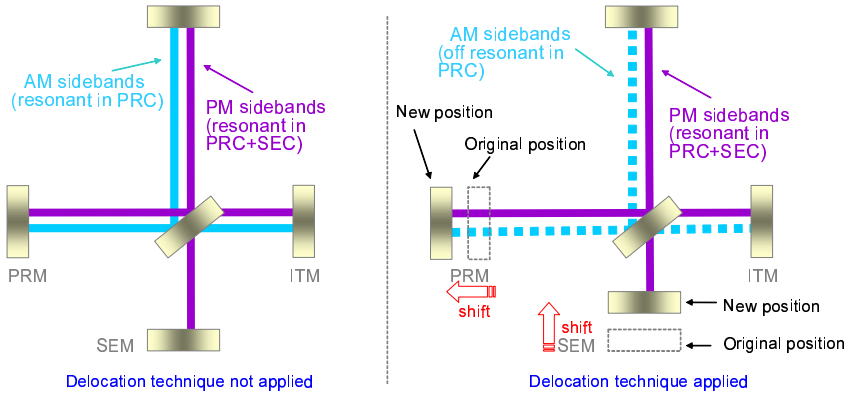

Figure 3. Central part with and without the delocation technique.

Table 1. Normalized control signal matrix

	$L+$	$L-$	$l+$	$l-$	ls
BP(SD)	1	8.0×10^{-6}	-2.6×10^{-2}	6.2×10^{-4}	1.3×10^{-2}
DP(SD)	-2.2×10^{-8}	1	1.4×10^{-8}	1.3×10^{-2}	2.0×10^{-8}
BP(DD)	-4.9×10^{-2}	-1.1×10^{-4}	1	-8.6×10^{-3}	-5.3×10^{-1}
DP(DD)	-1.0×10^{-4}	7.6×10^{-2}	1.4×10^{-3}	1	1.1×10^{-5}
PO(DD)	-1.5×10^{-1}	-1.2×10^{-2}	1.1	-2.2×10^{-2}	1

Table 2. Normalized diagonalized control signal matrix

	dem. phase	$l+$	$l-$	ls
PO(DD)	for $l+$	1	-4.2×10^{-3}	5.5×10^{-4}
DP(DD)	for $l-$	2.2×10^{-3}	1	-5.6×10^{-5}
PO(DD)	for ls	5.0×10^{-4}	-1.1×10^{-7}	1

3. Experimental status

In 2006 we designed and built a prototype tuned RSE interferometer inside the campus of National Astronomical Observatory of Japan(NAOJ). Figure 4 shows the optical layout of the prototype interferometer. All of the seven test masses are suspended as double pendulums to suppress the mirror motion at frequencies above the resonant frequency. The FP cavity finesse is 122. The test mass motion around its resonant frequency is damped by an eddy current damping system. The lock of the RSE has been successfully demonstrated. As of July 2007, the two Fabry-Perot cavities are individually controlled instead of controlling the $L+$ and the $L-$ DOFs which is the designed configuration. The lock is demonstrated without the delocation scheme at present. We define several lock states, which are shown in Fig. 5. Each state is indicated as follows.

- State 1 : Michelson is locked to dark fringe at the DP.
- State 2 : Power-recycled Michelson is locked.

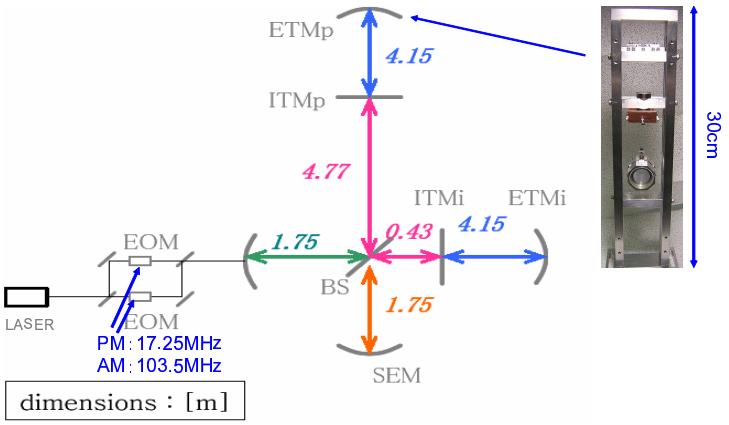

Figure 4. Optical layout of the prototype interferometer.

- State 3 : Central part is locked.
- State 4 : Tuned RSE is locked

In state 3, the carrier is not yet resonant inside the PRC. In order for the carrier to be resonant inside the PRC, the phase needs to be shifted by π inside the PRC. This happens when the carrier is resonant inside the FP cavities. Figure 6 shows the DC power detected at various ports, (i.e. DP, BP, PO, transmitted port for the inline FP cavity and for the perpendicular FP cavity.) Each lock state is separated with boxes with colors specified in Fig. 5. In order to verify the locking status, resonant conditions for the two sets of sidebands are monitored with optical spectrum analyzers placed at the DP and the PO. Figure 7 shows the output of the optical spectrum analyzers. The red curves are the output power at the PO and the blue curves are output power at the DP. Colored boxes indicate the lock state, as specified in Fig. 5. In state 1, neither the AM nor the PM sidebands are resonant. In state 2, the AM sidebands are resonant inside the PRC, thus there are resonant peaks of the AM sidebands detected at the PO. The PM sidebands are not yet resonant. In state 3, the PM sidebands are resonant inside the compound cavity made of the PRC and the SEC thus there are resonant peaks of the PM sidebands detected at the DP. Each cavity length is controlled throughout the locking process.

4. Summary and future work

A new control scheme of a tuned RSE configuration for next-generation gravitational-wave detectors was developed and has been tested with a prototype RSE interferometer. The lock of the tuned RSE interferometer has been successfully demonstrated. As of July 2007, the FP cavities are individually controlled, which differs from the final design which controls the common and the differential modes of the cavities. The next step is to demonstrate control using common and differential mode feedback and measure the sensing matrix. The delocation scheme can be tested once the designed sensing and control scheme has been successfully demonstrated, measured, and compared with modeling results.

4.1. Acknowledgments

This research is supported in part by a Grant-in-Aid for Scientific Research on Priority Areas (415) of the Ministry of Education, Culture, Sports, Science, and Technology, from Japan, and also partially supported by the US National Science Foundation under cooperative agreement PHY-0107417.

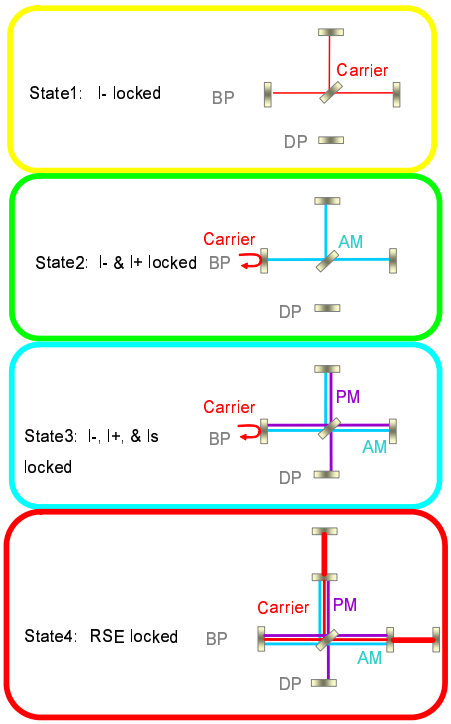

Figure 5. Lock states of the interferometer.

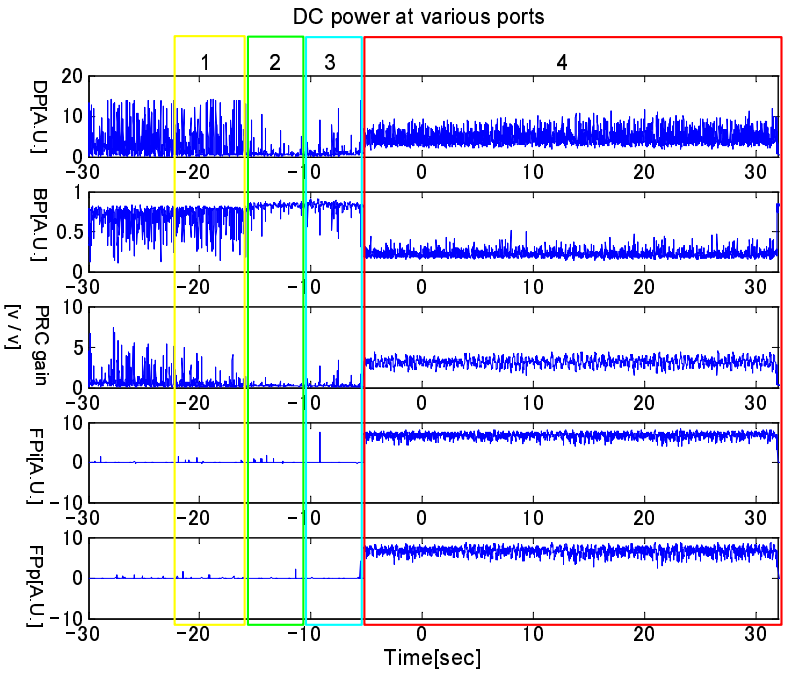

Figure 6. DC power at various ports.

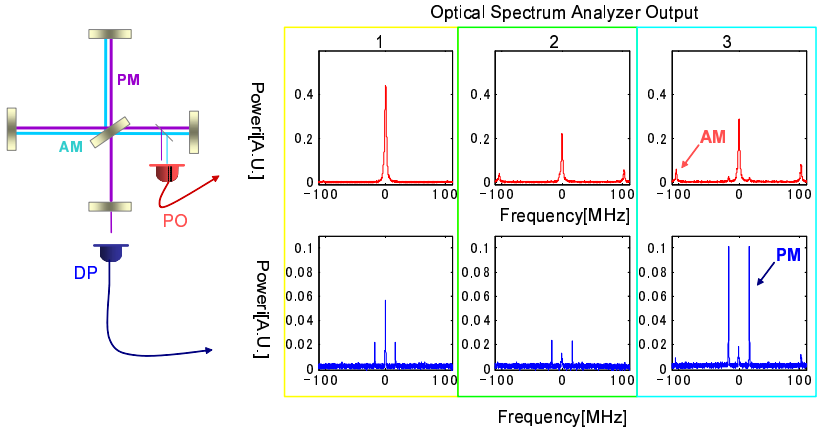

Figure 7. Sideband resonant peaks inside the PRC and the SEC.

References

[1] Sigg D *et al* 2006 *Class. Quantum. Grav.* **23** S51–S56
[2] Lück H *et al* 2006 *Class. Quantum Grav.* **23** S71–S78
[3] Qipiani K *et al* 2005 *Class. Quantum Grav.* **22** S869–S880.
[4] Ando M *et al* 2005 *Class. Quantum Grav.* **22** S881–S889
[5] Fritschel P 2003 *Proc. SPIE Int. Soc. Opt. Eng.* Vol. 4856, p. 282
[6] K. Kuroda *et al* 1999 *Int. J. Mod. Phys.* D 8, 557
[7] Kawazoe F *et al* 2007 *J. Phys.: Conf. Series* **32** 380–385
[8] Sato S *et al* 2007 *Phys. Rev.* D **75** 082004